



OPEN The effect of 2-Deoxy-D-glucose on glycolytic metabolism in acute myeloblastic leukemic ML-1 cells

Nichlas Vous Christensen, Johanne Haahr Knudsen, Christoffer Laustsen & Lotte Bonde Bertelsen ✉

Acute myeloblastic leukemia (AML) is one of the most common and life-threatening forms of leukemia. Treatment remains challenging due to its high heterogeneity, drug resistance, and metabolic flexibility. Targeting specific metabolic pathways has emerged as a promising therapeutic approach. The ability to monitor treatment response is crucial for disease management. Here, we utilized hyperpolarized ^{13}C nuclear magnetic resonance (NMR) spectroscopy to evaluate the therapeutic effects of 2-deoxy-D-glucose (2-DG), a glucose analog known to inhibit glycolysis and induce cell death in leukemic cell lines. Hyperpolarized ^{13}C NMR spectroscopy, biochemical assays, and respirometry were used to assess the metabolic effects of 2-DG treatment at various concentrations on the AML cell line ML-1 in vitro. Significant metabolic alterations were observed following 2-DG treatment at 2 mM and 5 mM for 24 h, as revealed by multiple analytical approaches. The concentration-dependent effects of 2-DG treatment were clearly detected using hyperpolarized NMR, demonstrating substantial inhibition of glycolytic pathways in ML-1 cells. This study supports the potential of 2-DG for enhancing chemosensitivity in AML treatment and highlights hyperpolarized NMR as a valuable tool for therapy evaluation.

Keywords AML, 2-DG, Glycolytic metabolism, Hyperpolarization, NMR

Abbreviations

AML	Acute myeloblastic leukemia
2-DG	2-Deoxy-D-glucose
ALL	Acute lymphoblastic leukemia
HP	Hyperpolarized
NMR	Nuclear Magnetic Resonance
PDH	Pyruvate dehydrogenase
LDH	Lactate dehydrogenase
HK	Hexokinase
RT-qPCR	Reverse transcription-quantitative polymerase chain reaction
RPL22	Ribosomal Protein L22
ECAR	Extracellular acidification rate
OCR	Oxygen consumption rate
SEM	Standard error of mean

Leukemia is a cancer that mostly originates in the bone marrow and leads to a high number of abnormal blood cells. Leukemia is classified into four major groups, where one group, the acute myeloblastic leukemia (AML) is one of the most common and life-threatening of leukemias¹. Treatment of AML has been a challenging task for several decades, due to its high heterogeneity, drug resistance and flexibility in its metabolic pathways^{1–3}. AML is metabolically altered (Warburg Effect), and targeting the cellular metabolism in treatment has shown promising results recently^{4,5}. However, due to AML's high metabolic diversity and plasticity, novel drugs that target the metabolic pathways are desperately needed.

2-Deoxy-D-glucose (2-DG) is a synthetic glucose analog that has shown potential as a potential therapeutic drug for various cancer treatments^{6–8}. Glucose transporters are usually highly upregulated in cancer cells which promotes the uptake of 2-DG⁷. 2-DG is phosphorylated by hexokinase II in the glycolysis and accumulates as 2-Dexoy-D-glucose-6-phosphat (2-DG-6-P) which cannot be further metabolized and can lead to cell starvation

Department of Clinical Medicine, MR Research Centre, Aarhus University, Palle Juul-Jensens Boulevard 99, Aarhus, Denmark. ✉email: lotte@clin.au.dk

and death^{9,10}. Despite its critical interference with metabolism, the glucose analog does not seem to impact normal tissue severely at lower concentrations¹¹. Acute lymphoblastic leukemia (ALL), another one of the major leukemia groups, has been shown to die after a low-dose treatment with 2-DG in vitro¹². Similar treatment protocols has been shown for various AML cell-lines in vitro, but often requiring higher concentrations to observe any reduction in metabolic activity^{13,14}. These earlier studies have been using AML cell-lines of various subtype origin from M1 to M6 in the FAB classification¹⁵. In this work, we investigated how the metabolism of the AML cell-line ML-1 was impacted by 2-DG treatment at various concentrations. ML-1 is a cell-line of the M4 subtype which has shown interesting metabolic properties and is considered a suitable test model for the study of drug intervention due to its high hormonal production¹⁶. The investigations were conducted using biochemical assays as well as hyperpolarized (HP) ¹³C Nuclear Magnetic Resonance (NMR) spectroscopy to determine changes in metabolic pathways and enzyme activity. HP ¹³C NMR has proven to be a promising tool in metabolic investigations both in vitro and in vivo due to its ability to monitor metabolic flux in real-time^{17–19}.

Methods and materials

Cells and treatment

ML-1 cells, a human AML cell-line, were obtained from Sigma-Aldrich (St. Louis, Missouri, USA). ML-1 cells were cultured in RPMI-1640 media (with 2 g/L glucose, L-glutamine, no sodium pyruvate) (Product R8758, Sigma-Aldrich, St. Louis, Missouri, USA) with 10% v/v heat Inactivated Fetal Bovine Serum and 1% v/v Penicillin–Streptomycin and was maintained in continuous culture at 37 °C in a humidified atmosphere (5% CO₂) in an incubator. Growth medium was changed every two to three days. The viability with and without treatment was determined through cell-counting with a trypan blue exclusion test. For this, the ML-1 cells were treated with 0, 2, 5, 10, 20, 40 and 100 mM 2-DG (n = 3 per group), respectively. The cells were counted using a Trypan blue exclusion test after 15 min, 30 min, 1 h, 3 h, 6 h, 24 h and 48 h. For all other experiments, three groups of cells were prepared; one group of cells was left untreated (denoted 0 mM), one group was treated with 2 mM 2-DG and one group was treated with 5 mM 2-DG. Treatments were for 24 h. Prior to any assay or HP experimentation the treated cells were centrifuged and redissolved in 2-DG free RPMI-1640 media.

Hyperpolarized NMR experiments with [1-¹³C]pyruvate

HP NMR experiments were performed on 0 mM (n = 6), 2 mM (n = 8) and 5 mM (n = 5) treated cells using both 60 and 43 MHz benchtop NMR spectrometers equipped with a ¹³C coil (Magritek, Wellington, New Zealand). [1-¹³C]pyruvate was polarized in either a SpinLab (GE Healthcare, Denmark) or in a SpinAligner (Polarize, Frederiksberg, Denmark) to achieve 20–60% polarization. Following dissolution in phosphate-buffer, HP pyruvate was added to 25 million cells in RPMI (1:10 dilution factor, resulting in a pyruvate concentration of 8 mM), and subsequently transferred to a 5 mm NMR tube and inserted into the spectrometer. A ¹³C single-pulse time-series was acquired with a 1-s repetition time over 5 min using a hard-pulse with a flip-angle of 10°.

Biochemical and gene expression analysis

Biochemical analysis of PDH and LDH enzyme activities as well as lactate concentrations was performed. The assays were performed according to the manufacturer's instructions with few alterations (Sigma-Aldrich, Copenhagen, Denmark). In brief, cells and medium were separated by centrifugation and samples stored at -80 °C until analysis. Analysis was performed in 384 well-plates in a microplate reader (SYNERGY H1; Biotek, Aarhus, Denmark). Activity measurements were normalized to total protein and protein quantification was performed utilizing a Qubit 3.0 fluorometer (Fisher Scientific, Wilmington, DE) (Table 1).

Expression of HK, LDH and PDH was quantified using RT-qPCR. RNA was extracted using TRIzol (ThermoFisher Scientific), and cDNA was synthesized (K1621, ThermoFisher Scientific). The Maxima SYBR Green/ROX qPCR Master Mix was used for qPCR (ThermoFisher Scientific). A melting curve analysis was conducted to ensure specificity and a standard curve was constructed by plotting threshold cycle (Ct values) against serial dilutions of purified PCR product. Expression was normalized to the RPL22 housekeeping gene. The following primer sequences were used:

Respirometry

Oxygen consumption rate (OCR) and Extracellular acidification rate (ECAR) were measured at 37 °C in a closed Unisense micro-respiration chamber with an O₂-electrode (Unisense A/S, Aarhus, Denmark). For each experiment, 30 million ML-1 cells in suspension were used. Cells were resuspended in DMEM medium (glucose- and sodium pyruvate-free) (Product 11,966,025, Fisher Scientific, Hampton, New Hampshire, USA) and transferred to a closed chamber and allowed to stabilize for 15 min before the start of measurement. After stabilization, cells were sequentially exposed to glucose (50 mM), oligomycin (5 μM), and 2-DG (100 mM) and antimycin A (4 μM). Measurements were performed for 20 min after each injection.

Gene	Forward primer sequence	Reverse primer sequence
RPL22	5'-GGAGCAAGAGCAAGATCACC -3'	5'-TGTTAGCAACTACGCGCAAC-3'
LDHA	5'-GAAAGCTGTTCATGGGCTGAT-3'	5'-GTGGACATTTTCCCACTGCT-3'
PDH	5'-AGAACTTCTACGGGGGCAAT -3'	5'-CGAATATCTGGCCCTGGTTA-3'
HK	5'-GGA CTG GAC CGT CTG AAT GT -3'	5'-ACA GTT CCT TCA CCG TCT GG -3'

Table 1. Primers for qPCR.

Data processing and statistics

HP time-series data were analyzed with iNMR (Nucleomatica, Molfetta, Italy). Lactate-to-all-carbon ratios were extracted from the summed time-series. Note that only the downstream product lactate was observed, so lactate-to-all-carbon directly correlates to lactate-to-pyruvate. All data are presented as mean and standard error of mean (SEM). All statistical analysis were performed in GraphPad Prism 10. Data were analyzed with a one-way or two-way ANOVA followed by Dunnett's multiple comparison test unless otherwise specified to be Tukey's multiple comparisons test. An unpaired t-test was also used. *p*-values below 0.05 (*) were considered statistically significant.

Results

Proliferation

ML-1 cell proliferation as determined by trypan blue exclusion tests at various 2-DG treatment concentrations and durations can be seen in Fig. 1. No significant differences were observed between treatment concentrations at 6 h. However, two-way ANOVA without repeated measures revealed that cell growth was significantly inhibited ($F(2, 24) = 14.84, p < 0.0001$) at concentrations ≥ 5 mM after 24 h (Tukey's: $p = 0.0326$) and at concentrations ≥ 2 mM after 48 h (Tukey's: $p < 0.0001$). Figure 1B specifically shows cell growth for 0, 2, and 5 mM after 24 h. These treatment conditions were used for subsequent experiments, as they provided a measurable effect without causing excessive toxicity. Cell viability, quantified as the ratio of live and dead cells in the trypan blue exclusion test, can be seen in Fig. 1C. One-way ANOVA revealed no significant differences between the different treatment schemes ($F(2, 6) = 3.226, p = 0.1119$).

Hyperpolarized [^{13}C] pyruvate conversion

To assess the more immediate effects of 2-DG treatment, such as metabolic changes, hyperpolarization experiments were performed on cells treated with different 2-DG concentrations. The results of the hyperpolarization experiments can be seen in Fig. 2 along with an illustration of relevant metabolic pathways of the glycolysis. The [^{13}C]pyruvate to [^{13}C]lactate flux was significantly lowered after 5 mM 2-DG treatment for 24 h, see Fig. 2B. This showcases the impact that 2-DG could have on metabolism, as illustrated in Fig. 2A. The inhibition of glycolysis by 2-DG could potentially affect downstream processes and enzymes, such as LDH, as the cells experience starvation. Unlike proliferation and viability, which showed no immediate changes, the

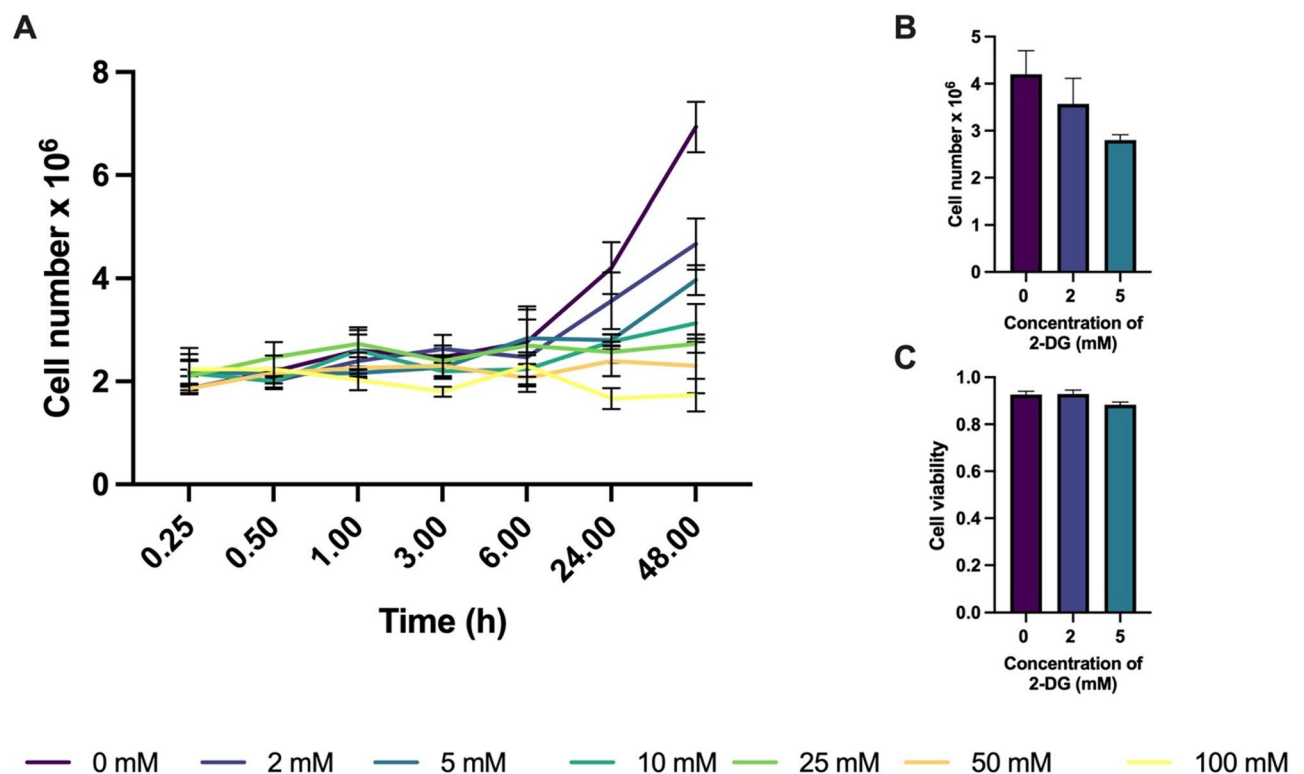


Fig. 1. (A) Cell proliferation as a function of 2-DG treatment duration at various concentrations ranging from 0 to 100 mM ($n = 3$ for each group). Each sample started with 5 million cells at $t = 0$. Note that the time axis is not to scale. (B) Cell proliferation at 24 h specifically for 0, 2 and 5 mM 2-DG treatment. One-way ANOVA determined no statistical significance ($F(2, 6) = 2.597, p = 0.1540$). (C) Cell viability after 24 h for 0, 2 and 5 mM 2-DG treatment. One-way ANOVA determined no statistical significance ($F(2, 6) = 3.226, p = 0.1119$). The mean \pm SEM are shown for each group.

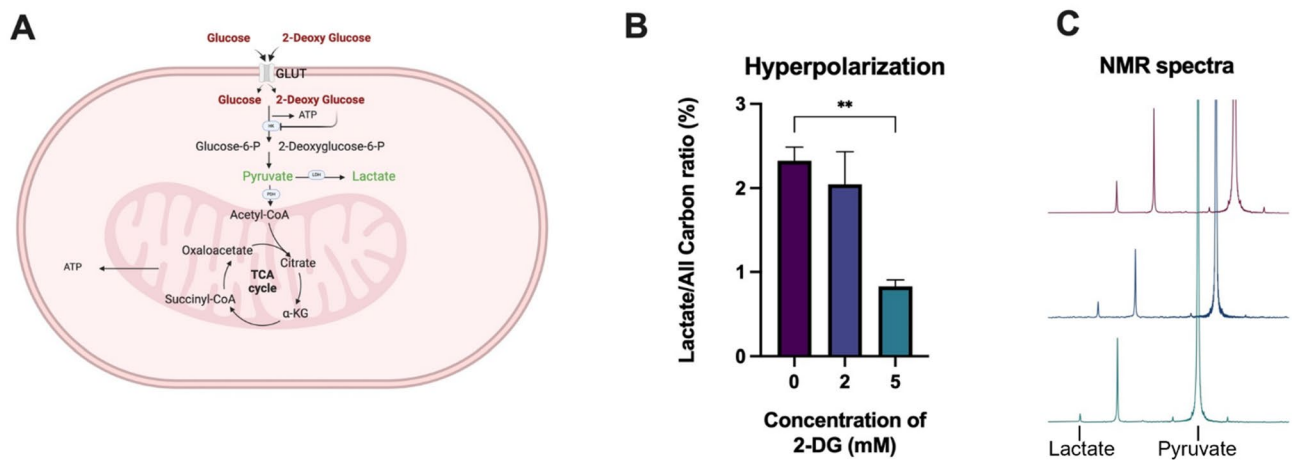


Fig. 2. (A) Schematic illustration of 2-DG inhibition in the glycolysis and metabolic flux of HP pyruvate. 2-DG inhibits glycolysis by targeting hexokinase (HK), thereby limiting the utilization of normal glucose. Illustration was created using BioRender.com. (B) Resulting lactate-to-all-carbon ratios at 0 (n = 6), 2 (n = 8) and 5 (n = 5) mM 2-DG treatment for 24 h. The mean \pm SEM are shown for each group. One-way ANOVA determined statistical significance between groups ($F(2,16) = 5.87, p = 0.0123$). Statistical significance is marked (** $p < 0.01$). The ratios were computed from summed time-series data. (C) Sum of NMR time-series from the hyperpolarized experiments shown with one representative example in each treatment group.

pyruvate-to-lactate flux exhibited a measurable reduction after 24 h of treatment. This suggests that metabolic alterations occur before macroscopic cellular changes become apparent.

Biochemical assays

To further evaluate the impact of 2-DG treatment on metabolism, various biochemical assays were performed (Fig. 3). Gene expression analysis (Fig. 3A) revealed a significant reduction in PDH and HK mRNA expression. According to the ANOVA, the LDH expression was not statistically significant but showed a tendency to decrease already upon treatment with 2 mM 2-DG. When data are pooled into the two categories 0 mM and > 2 mM and analyzed using an unpaired t-test, a significant difference emerges ($p = 0.0121$). This suggests that the low sample size may obscure effects in the ANOVA, and that LDH expression is indeed significantly affected by 2-DG treatment, despite the lack of significance across all three conditions in the ANOVA. Neither the PDH nor the LDH activity were significantly impacted by the treatment schemes (Fig. 3B-C). Note here that the enzymatic activities are normalized to total protein and are thus not a measure of absolute activity. Finally, lactate concentrations (Fig. 3D) confirmed that basal glycolysis was inhibited by 2-DG treatment, as observed in HP experiments. Both 2 mM and 5 mM treatments resulted in a significant reduction in lactate concentrations.

Respirometry

We assessed glycolytic function in both untreated and 2-DG-treated cells, allowing us to measure and calculate various parameters such as basal glycolysis, glycolytic capacity, and OCR (Fig. 4). When ML-1 cells were treated with 5 mM 2-DG, both the basal glycolysis and the glycolytic capacity were significantly reduced, as measured by ECAR. Glycolytic capacity differs from basal glycolysis in that it represents the maximum rate of glucose-to-pyruvate/lactate conversion, measured after oligomycin inhibition of oxidative phosphorylation (OXPHOS), forcing the cell to rely solely on glycolysis for ATP production. As shown in Fig. 4B, OCR was also significantly reduced following both 2 mM and 5 mM 2-DG treatments. Interestingly, after glucose exposure, OCR increased only in untreated cells, suggesting that treated cells were unable to effectively utilize the supplied glucose due to competitive inhibition of hexokinase by 2-DG-6-P. Furthermore, additional 2-DG exposure appeared to have a greater impact on treated cells than on untreated ones, likely due to complete hexokinase inhibition.

Discussion

From the various experiments performed in this work, we explored the impact of 2-DG treatment on glycolytic activity in the AML cell-line ML-1. As evident from the hyperpolarized experiments and biochemical assays, the glycolytic activity (both glucose and pyruvate consumption) was significantly inhibited after treatment with 5 mM 2-DG for 24 h, and moderately inhibited after 2 mM 2-DG treatment for 24 h. For comparison, Gu et al.¹² found that 1 mM 2-DG treatment was sufficient to induce cell death in various ALL cell-lines in vitro. Lapa et al.¹⁴ found 2-DG concentrations to vary from 3.7 mM to 9.5 mM in order to reduce metabolism by 50% in various AML cell-lines in vitro (THP-1, HL-60, K-562, HEL, NB-4 and KG-1). Our findings align with these reports, showing that similar concentration levels were needed to reduce metabolism in the ML-1 cell-line specifically. Extracellular glucose concentration also plays a crucial role in 2-DG uptake, as both glucose and 2-DG compete for the same GLUT-1 transporter. In our study, ML-1 cells were cultured in RPMI medium containing 11 mM glucose, which mirrors typical in vivo concentrations (5–10 mM). This concentration

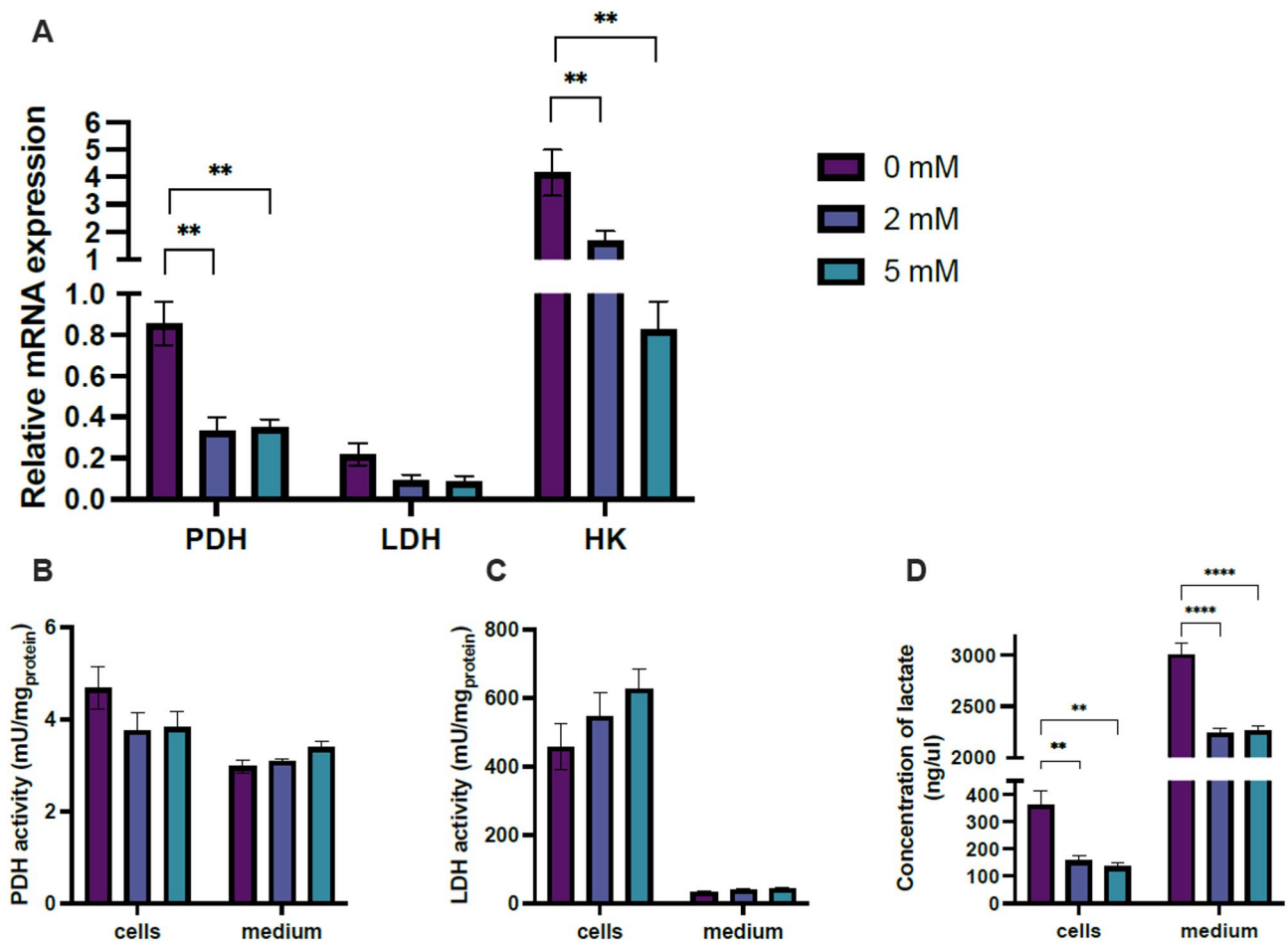


Fig. 3. Biochemical assays to access lactate concentration, LDH activity, mRNA expression and PDH activity were performed on cells with 0, 2 and 5 mM 2-DG treatment for 24 h. **(A)** qPCR measured the relative mRNA expression of three relevant enzymes, namely PDH, LDH and HK. One-way ANOVA determined statistical significance between groups for PDH and HK: $F(2, 9) = 15.9, p = 0.0011$ and $F(2, 9) = 12.9, p = 0.0023$, respectively. For LDH there was no statistical significance ($F(2, 9) = 4.4, p = 0.0518$). **(B)** PDH activity in cells and in medium. Two-way ANOVA determined no statistical significance between treatment groups ($F(2, 24) = 2.6, p = 0.0925$). **(C)** LDH activity in cells and in medium. Two-way ANOVA determined no statistical significance between treatment groups ($F(2, 24) = 1.4, p = 0.2550$). **(D)** Lactate concentration in the cells and in medium. Two-way ANOVA determined statistical significance between treatment groups ($F(2, 24) = 14.84, p < 0.0001$). The mean \pm SEM are shown for each group ($n = 5$). Statistical significance is marked on figures (** $p < 0.01$, **** $p < 0.0001$).

reflects physiological conditions and impacts 2-DG effectiveness. Previous studies have shown that normal glucose levels enhance 2-DG uptake compared to hyperglycemic conditions, as demonstrated in rodent models using 2-[F-18]-fluoro-2-deoxy-D-glucose²¹. These findings suggest that normal serum glucose levels facilitate sufficient 2-DG accumulation for treatment.

HK and GLUT-1 have been shown to be upregulated in AML compared to non-leukemic cells, especially in drug-resistant subtypes^{22,23}. Similarly, ALL cells typically exhibit increased HK expression¹². This upregulation drives high glucose uptake and glycolytic activity, making glycolysis an attractive therapeutic target. In our study, we observed a marked reduction in hexokinase mRNA expression following 2-DG treatment, which we interpret as a response to severe metabolic stress and glucose deprivation. Although apoptosis per se does not necessarily lead to decreased HK expression, the reduction in HK expression is consistent with a metabolic shutdown triggered by glucose deprivation, a well-known stimulus for apoptotic signaling¹⁰. Also, given that LDH expression often is upregulated in rapidly proliferating and glycolysis-dependent cells, its reduction aligns with metabolic arrest. Although cell viability appeared unaffected in the trypan blue exclusion test (which is limited in its ability to distinguish early apoptotic cells²⁴), the overall metabolic indicators strongly suggest that 2-DG treatment drives ML-1 cells toward an apoptotic or pre-apoptotic state.

In HP experiments, pyruvate conversion to lactate and bicarbonate reflects glycolytic and oxidative fluxes, respectively. Lactate formation aligns with ECAR (anaerobic glycolysis), while bicarbonate (though not observed in our HP data) would link to OCR (oxidative metabolism). A high lactate/pyruvate ratio suggests dominant glycolysis (high ECAR, low OCR), characteristic of the Warburg effect or hypoxia. Now, 2-DG in treated cells

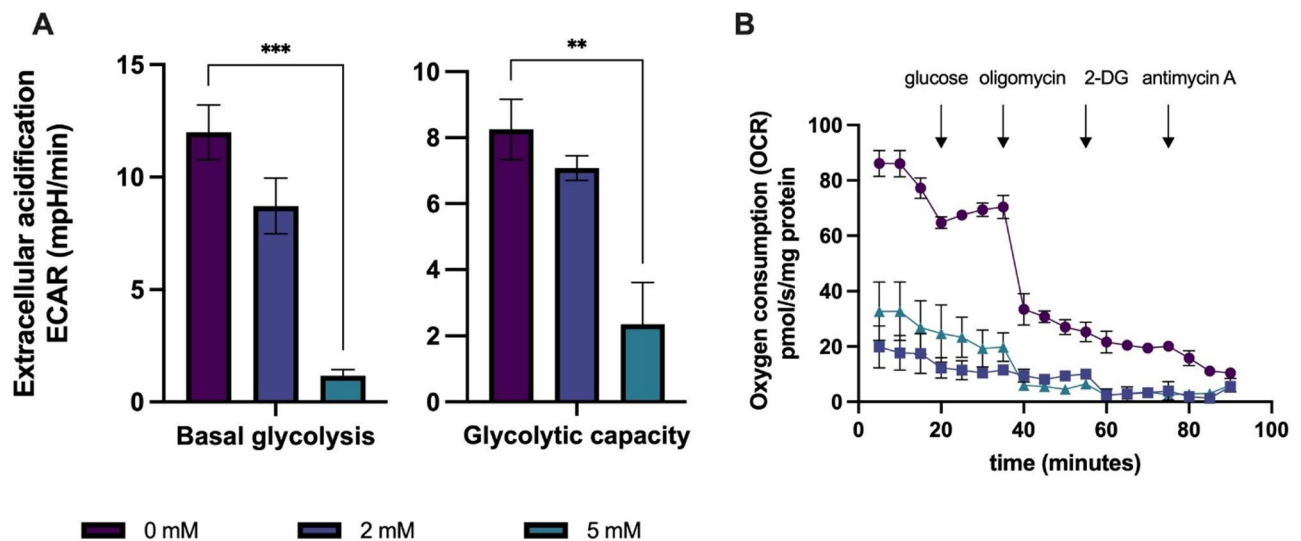


Fig. 4. (A) ECAR (mpH/min) in 0 mM ($n = 3$), 2 mM ($n = 3$) and 5 mM ($n = 3$) 2-DG treated cells for 24 h. One-way ANOVA determined statistical significance between treatment groups: $F(2, 6) = 29.7$, $p = 0.0008$ and $F(2, 6) = 11.4$, $p = 0.0090$ for basal glycolysis and glycolytic capacity, respectively. (B) OCR in response to glucose, oligomycin and 2-DG exposure. Each data point represents mean \pm SEM. Statistical significance is marked (** $p < 0.01$, *** $p < 0.001$).

accumulates as the metabolic 2-DG-6-P product which inhibits hexokinase by competitive binding²⁵. The impact of this inhibition becomes clear when examining the OCR data in Fig. 4. The exposure to a high dose of 2-DG (100 mM) appears to halt overall metabolism in treated cells, effectively suppressing OCR, while nontreated cells remain only mildly affected. This effect may be attributed to the already-high accumulation of 2-DG-6-P in treated cells. The rapid saturation of 2-DG-6-P likely prevents further glycolytic flux, reinforcing the metabolic blockade observed in ECAR and OCR measurements.

Cells that rely heavily on glycolysis, as many cancers do, can be majorly impacted by 2-DG treatment. However, other cell-line models, such as the AML-M5 subtype, have been shown to favor fatty acid metabolism for supply of metabolites in the TCA and subsequent OXPHOS²⁶. This metabolic preference makes AML-M5 cells less susceptible to starvation under 2-DG treatment, thereby increasing their resistance. Cells with high metabolic diversity and plasticity may shift from glycolysis dependence to fatty acid dependence during a glycolysis inhibiting treatment. This metabolic adaptation could potentially be observed using HP probes that track both glycolytic metabolism ([1-¹³C]pyruvate) and fatty acid metabolism ([1-¹³C]acetate)²⁷.

Although lactate metabolism do not necessarily correlate directly with treatment efficacy as cancer cells could exhibit various metabolic adaptations, the use of HP tracers to measure treatment response has previously been demonstrated in several studies in both animal models and patients^{28–30}. Our study did not demonstrate HP NMR to be a superior predictor of treatment response compared to other conventional cell assessment methods. However, it provides an alternative approach which allows direct assessment on live cells both in vitro and in vivo. Using HP methods to monitor lactate flux changes, oncologists could assess a tumor's response to treatment within hours of administering a HP compound. If the tumor responds favorably, the current treatment can continue. However, if little to no response is detected, oncologists may consider alternative, potentially more effective therapies. This early-response assessment could transform cancer treatment by enabling timely adjustments based on real-time metabolic feedback. Such an approach may lead to more personalized and effective treatment strategies, improving patient outcomes and accelerating drug development.

Important to note is that the high 2-DG concentrations used in our experiments are not intended for direct clinical application due to known toxicity concerns¹¹. Instead, we employed 2-DG as a proof-of-concept tool to monitor glycolysis targeting in leukemia cells. Although 2-DG is a well-established glycolysis inhibitor, its clinical use is limited by toxicity, highlighting the need for developing new, less toxic agents—potentially in combination with co-drugs—to achieve similar metabolic effects. Similar to previous in vitro studies^{31–33}, our study also demonstrates the utility of HP NMR in tracking metabolic changes, paving the way for future in vivo validations and the development of improved drugs for clinical application.

In summary, this work offers a novel contribution by demonstrating how hyperpolarized ¹³C NMR can be applied to assess early metabolic responses to glycolytic inhibition in a leukemia model. While hyperpolarized NMR has been used in oncology research before, its application in the evaluation of drug effects in AML remains limited. And while our approach also builds on established methodologies, it extends them by incorporating a concentration-dependent evaluation of a glycolysis inhibitor across multiple analytical platforms. This enables the detection of subtle yet biologically relevant metabolic changes. In this regard, the study contributes to the evolving application of hyperpolarized NMR in drug response assessment, and suggests its potential utility for early, functional readouts of treatment effect.

Conclusion

2-DG inhibited cell proliferation, anaerobic glycolysis, and OXPHOS in ML-1 cells. The concentration-dependent effects of 2-DG treatment were clearly observed using HP ^{13}C NMR. This study supports previous findings on the potential of 2-DG for enhancing chemosensitivity in AML treatment and also highlights hyperpolarized NMR as a valuable tool for therapy evaluation.

Data availability

The data presented in this work is available upon reasonable request. Contact Lotte Bonde Bertelsen at lotte@clin.au.dk.

Received: 11 February 2025; Accepted: 6 May 2025

Published online: 21 May 2025

References

- Kreitz, J. et al. Metabolic plasticity of acute myeloid leukemia. *Cells* **8**(8), 1–28. <https://doi.org/10.3390/cells8080805> (2019).
- Burnett, A. K. The treatment of AML: Current status and novel approaches. *Hematology* **10**(SUPPL. 1), 50–53. <https://doi.org/10.1080/10245330512331389773> (2005).
- Shaffer, B. C. et al. Drug resistance: Still a daunting challenge to the successful treatment of AML. *Drug Resist. Updates* **15**(1), 62–69. <https://doi.org/10.1016/j.drug.2012.02.001> (2012).
- Grønningssæter, I. S. et al. Targeting cellular metabolism in acute myeloid leukemia and the role of patient heterogeneity. *Cells* <https://doi.org/10.3390/cells9051155> (2020).
- Short, N. J. et al. Advances in the treatment of acute myeloid leukemia: New drugs and new challenges. *Cancer Discov.* **10**(4), 506–525. <https://doi.org/10.1158/2159-8290.CD-19-1011> (2020).
- Zhang, D. et al. 2-Deoxy-D-glucose targeting of glucose metabolism in cancer cells as a potential therapy. *Cancer Lett.* **355**(2), 176–183. <https://doi.org/10.1016/j.canlet.2014.09.003> (2014).
- Pajak, B. et al. 2-Deoxy-D-glucose and its analogs: From diagnostic to therapeutic agents. *Int. J. Mol. Sci.* <https://doi.org/10.3390/ijms21010234> (2020).
- Singh, R., Gupta, V., Kumar, A. & Singh, K. 2-Deoxy-D-glucose: A novel pharmacological agent for killing hypoxic tumor cells, oxygen dependence-lowering in Covid-19, and other pharmacological activities. *Adv. Pharmacol. Pharm. Sci.* <https://doi.org/10.1155/2023/9993386> (2023).
- Aft, R. L., Zhang, F. W. & Gius, D. Evaluation of 2-deoxy-D-glucose as a chemotherapeutic agent: Mechanism of cell death. *Br. J. Cancer* **87**(7), 805–812. <https://doi.org/10.1038/sj.bjc.6600547> (2002).
- Pelicano, H., Martin, D. S., Xu, R. H. & Huang, P. Glycolysis inhibition for anticancer treatment. *Oncogene* **25**(34), 4633–4646. <https://doi.org/10.1038/sj.onc.1209597> (2006).
- Farooque, A., Afrin, F., Adhikari, J. S. & Dwarakanath, B. S. Protection of normal cells and tissues during radio- and chemosensitization of tumors by 2-deoxy-D-glucose. *J. Cancer Res. Ther.* **5**(Suppl 1), S32–5. <https://doi.org/10.4103/0973-1482.55138> (2009).
- Gu, L. et al. Low dose of 2-deoxy-D-glucose kills acute lymphoblastic leukemia cells and reverses glucocorticoid resistance via N-linked glycosylation inhibition under normoxia. *Oncotarget* **8**(19), 30978–30991. <https://doi.org/10.18632/oncotarget.16046> (2017).
- Larrue, C. et al. Antileukemic activity of 2-Deoxy-d-glucose through inhibition of n-linked glycosylation in acute myeloid leukemia with FLT3-ITD or c-KIT mutations. *Mol. Cancer Ther.* **14**(10), 2364–2373. <https://doi.org/10.1158/1535-7163.MCT-15-0163> (2015).
- Lapa, B. et al. Acute myeloid leukemia sensitivity to metabolic inhibitors: glycolysis showed to be a better therapeutic target. *Med. Oncol.* **37**(8), 72. <https://doi.org/10.1007/s12032-020-01394-6> (2020).
- Muniraj, F. Classification of acute leukemias – past, present, and future. *IJSS Case Rep. Rev.* **1**(12), 61–66. <https://doi.org/10.17354/cr/2015/93> (2015).
- Schönberger, J. et al. Establishment and characterization of the follicular thyroid carcinoma cell line ML-1. *J. Mol. Med* **78**(2), 102–110. <https://doi.org/10.1007/s001090000085> (2000).
- Wang, Z. J. et al. Hyperpolarized ^{13}C MRI: State of the art and future directions. *Radiology* **291**(2), 273–284. <https://doi.org/10.1148/radiol.2019182391> (2019).
- Harris, T. et al. Hyperpolarized product selective saturating-excitations for determination of changes in metabolic reaction rates in real-time. *NMR Biomed.* **33**(2), 1–15. <https://doi.org/10.1002/nbm.4189> (2020).
- R. L. Hesketh, A. J. Wright, and K. M. Brindle, *Innovating metabolic biomarkers for hyperpolarized NMR BT - dynamic hyperpolarized nuclear magnetic resonance*, T. Jue and D. Mayer, Eds., Cham: Springer International Publishing, 2021, pp. 151–179. https://doi.org/10.1007/978-3-030-55043-1_7.
- Vogel, C. et al. Sequence signatures and mRNA concentration can explain two-thirds of protein abundance variation in a human cell line. *Mol. Syst. Biol.* **6**(1), 400. <https://doi.org/10.1038/msb.2010.59> (2010).
- Wahl, R. L., Henry, C. A. & Ethier, S. P. Serum glucose: effects on tumor and normal tissue accumulation of 2-[F-18]-fluoro-2-deoxy-D-glucose in rodents with mammary carcinoma. *Radiology* **183**(3), 643–647. <https://doi.org/10.1148/radiology.183.3.1584912> (1992).
- Song, K. et al. Resistance to chemotherapy is associated with altered glucose metabolism in acute myeloid leukemia. *Oncol. Lett.* **12**(1), 334–342. <https://doi.org/10.3892/ol.2016.4600> (2016).
- Miwa, H. et al. Leukemia cells demonstrate a different metabolic perturbation provoked by 2-deoxyglucose. *Oncol. Rep.* **29**(5), 2053–2057. <https://doi.org/10.3892/or.2013.2299> (2013).
- A. Ude, K. Afi-Leslie, K. Okeke, and E. Ogbodo, “Trypan Blue Exclusion Assay, Neutral Red, Acridine Orange and Propidium Iodide,” in *Cytotoxicity*, A. Sukumaran and M. A. Mansour, Eds., Rijeka: IntechOpen, 2022, ch. 8. <https://doi.org/10.5772/intechopen.105699>.
- Wijayasinghe, Y. S. et al. A comprehensive biological and synthetic perspective on 2-Deoxy-d-glucose (2-DG), a sweet molecule with therapeutic and diagnostic potentials. *J. Med. Chem.* **65**(5), 3706–3728. <https://doi.org/10.1021/acs.jmedchem.1c01737> (2022).
- Chen, M., Tao, Y., Yue, P., Guo, F. & Yan, X. Construction and validation of a fatty acid metabolism risk signature for predicting prognosis in acute myeloid leukemia. *BMC Genom. Data* **23**(1), 85. <https://doi.org/10.1186/s12863-022-01099-x> (2022).
- Bastiaansen, J. A. M. et al. 2013, “In vivo enzymatic activity of acetylCoA synthetase in skeletal muscle revealed by ^{13}C turnover from hyperpolarized [1- ^{13}C]acetate to [1- ^{13}C]acetylcarnitine”. *Biochimica et Biophysica Acta (BBA) General Subjects* **8**, 4171–4178 (1830).
- Woitek, R. et al. Hyperpolarized ^{13}C MRI of tumor metabolism demonstrates early metabolic response to neoadjuvant chemotherapy in breast cancer. *Radiol. Imaging Cancer* **2**(4), e200017. <https://doi.org/10.1148/rycan.2020200017> (2020).

29. Joergensen, S. H. et al. Hyperpolarized [1-13C]pyruvate cardiovascular magnetic resonance imaging identifies metabolic phenotypes in patients with heart failure. *J. Cardiovasc. Magn. Reson.* **26**(2), 101095. <https://doi.org/10.1016/j.jocmr.2024.101095> (2024).
30. Day, S. E. et al. Detecting tumor response to treatment using hyperpolarized 13C magnetic resonance imaging and spectroscopy. *Nat. Med.* **13**(11), 1382–1387. <https://doi.org/10.1038/nm1650> (2007).
31. Cavallari, E. et al. In-vitro NMR studies of prostate tumor cell metabolism by means of hyperpolarized [1–13C] pyruvate obtained using the PHIP-SAH method. *Front. Oncol.* <https://doi.org/10.3389/fonc.2020.00497> (2020).
32. Sriram, R. et al. Real-time measurement of hyperpolarized lactate production and efflux as a biomarker of tumor aggressiveness in an MR compatible 3D cell culture bioreactor. *NMR Biomed.* **28**(9), 1141–1149. <https://doi.org/10.1002/nbm.3354> (2015).
33. Christensen, N. V., Laustsen, C. & Bertelsen, L. B. Differentiating leukemia subtypes based on metabolic signatures using hyperpolarized 13C NMR. *NMR Biomed.* **37**(12), e5264. <https://doi.org/10.1002/nbm.5264> (2024).

Acknowledgements

This work is funded by Karen Elise Jensen Fonden (2020).

Author contributions

NVC: Data Curation, Formal analysis, Writing—Original Draft, Visualization. JHK: Investigation, Data curation, Writing—Reviewing and Editing. CL: Conceptualization, Methodology, Writing—Reviewing and Editing. LBB: Conceptualization, Methodology, Writing—Reviewing and Editing, Supervision, Data Curation, Formal analysis, Funding acquisition.

Declarations

Competing interests

The authors declare no competing interests.

Additional information

Correspondence and requests for materials should be addressed to L.B.B.

Reprints and permissions information is available at www.nature.com/reprints.

Publisher's note Springer Nature remains neutral with regard to jurisdictional claims in published maps and institutional affiliations.

Open Access This article is licensed under a Creative Commons Attribution-NonCommercial-NoDerivatives 4.0 International License, which permits any non-commercial use, sharing, distribution and reproduction in any medium or format, as long as you give appropriate credit to the original author(s) and the source, provide a link to the Creative Commons licence, and indicate if you modified the licensed material. You do not have permission under this licence to share adapted material derived from this article or parts of it. The images or other third party material in this article are included in the article's Creative Commons licence, unless indicated otherwise in a credit line to the material. If material is not included in the article's Creative Commons licence and your intended use is not permitted by statutory regulation or exceeds the permitted use, you will need to obtain permission directly from the copyright holder. To view a copy of this licence, visit <http://creativecommons.org/licenses/by-nc-nd/4.0/>.

© The Author(s) 2025